

AD-A101 611

UTAH UNIV SALT LAKE CITY DEPT OF CHEMISTRY

F/6 11/9

MEASUREMENTS OF THE PHOTOELASTIC AND ELASTIC CONSTANTS OF DRAWN—ETC(U)

JUN 81 D B CAVANAUGH, C H WANG

N00014-79-C-0507

NL

UNCLASSIFIED TR-6

1 OF 1
4D A
(081)

END
DATE
FILED
8-81
DTIC

AD A101611

SECURITY CLASSIFICATION OF THIS PAGE (When Data Entered)

REPORT DOCUMENTATION PAGE			READ INSTRUCTIONS BEFORE COMPLETING FORM	
1. REPORT NUMBER	2. GOVT ACCESSION NO.	3. RECIPIENT'S CATALOG NUMBER		
Technical Report #6	AD-A101611			
4. TITLE (and Subtitle) Measurements of the Photoelastic and Elastic Constants of Drawn Films and Extruded Rods of Polypropylene with Brillouin Light Scattering,			5. TYPE OF REPORT & PERIOD COVERED Technical Report.	
7. AUTHOR(s) David B. Cavanaugh and C. H. Wang			6. PERFORMING ORG. REPORT NUMBER	
8. PERFORMING ORGANIZATION NAME AND ADDRESS Department of Chemistry University of Utah Salt Lake City, Utah 84112			10. PROGRAM ELEMENT, PROJECT, TASK AREA & WORK UNIT NUMBERS	
11. CONTROLLING OFFICE NAME AND ADDRESS Office of Naval Research 800 N. Quincy St., Arlington, Va. 22217			12. REPORT DATE Jun 1981	
14. MONITORING AGENCY NAME & ADDRESS (if different from Controlling Office)			13. NUMBER OF PAGES 14	
16. DISTRIBUTION STATEMENT (of this Report)			15. SECURITY CLASS. (of this report) Unclassified	
17. DISTRIBUTION STATEMENT (of the abstract entered in Block 20, if different from Report)			15a. DECLASSIFICATION/DOWNGRADING SCHEDULE	
18. SUPPLEMENTARY NOTES Prepared for publication in the Journal of Applied Physics				
19. KEY WORDS (Continue on reverse side if necessary and identify by block number) Brillouin Scattering Spectra Structured polypropylene films and extruded rods Photoelastic constants, elastic constants Polymer morphology				
20. ABSTRACT (Continue on reverse side if necessary and identify by block number) The elastic constants C_{11} , C_{33} , C_{44} , C_{13} of oriented poly(propylene) films are measured with Brillouin scattering and are compared with the elastic constants obtained from extruded poly(propylene) rods. The photoelastic constants P_{12} , P_{13} and P_{31} of the extruded rod samples are measured by comparison to a poly(methylmethacrylate) reference scatterer. In the film samples, the relative values of the photoelastic constants P_{11} , P_{33} , P_{13} and P_{31} are measured by				

DD FORM 1 JAN 73 1473

EDITION OF 1 NOV 65 IS OBSOLETE
S/N 0102-LF-014-6601

SECURITY CLASSIFICATION OF THIS PAGE (When Data Entered)

81 7 17 128

SECURITY CLASSIFICATION OF THIS PAGE (When Data Entered)

20. comparison of the quasilongitudinal and quasitransverse intensities at several directions of sound propagation. Within the experimental error, P_{13} , P_{31} and P_{12} are found to be unaffected by extrusion or stretching. P_{11} and P_{33} are found to change in relation to P_{31} in the film samples. The results are interpreted by considering the chain morphology and the theory of photoelastic interaction. The changes in the Brillouin intensities are due to changes in the elastic constants rather than due to the photoelastic constants.

SECURITY CLASSIFICATION OF THIS PAGE (When Data Entered)

OFFICE OF NAVAL RESEARCH
Contract N00014 79C 0507
Serial RC-607

Technical Report No. 6

Measurements of the Photoelastic and Elastic
Constants of Drawn Films and Extruded Rods of
Polypropylene With Brillouin Light Scattering

by

David B. Cavanaugh and C. H. Wang

Department of Chemistry
University of Utah
Salt Lake City, Utah 84112

Prepared for Publication
in the
Journal of Applied Physics

June 26, 1981

Reproduction in whole or in part is permitted for any purpose of the
United States Government.

This document has been approved for public release; its distribution
is unlimited.

MEASUREMENTS OF THE PHOTOELASTIC AND ELASTIC
CONSTANTS OF DRAWN FILMS AND EXTRUDED RODS OF
POLYPROPYLENE WITH BRILLOUIN LIGHT SCATTERING

By

David B. Cavanaugh and C.H. Wang

University of Utah
Department of Chemistry
Salt Lake City, Utah 84112

ABSTRACT

The elastic constants C_{11} , C_{33} , C_{44} , C_{13} of oriented poly(propylene) films are measured with Brillouin scattering and are compared with the elastic constants obtained from extruded poly(propylene) rods. The photoelastic constants p_{12} , p_{13} and p_{31} of the extruded rod samples are measured by comparison to a poly(methylmethacrylate) reference scatterer. In the film samples, the relative values of the photoelastic constants p_{11} , p_{33} , p_{13} and p_{31} are measured by comparison of the quasilongitudinal and quasitransverse intensities at several directions of sound propagation. Within the experimental error, p_{13} , p_{31} and p_{12} are found to be unaffected by extrusion or stretching. p_{11} and p_{33} are found to change in relation to p_{31} in the film samples. The results are interpreted by considering the chain morphology and the theory of photoelastic interaction. The changes in the Brillouin intensities are due to changes in the elastic constants rather than due to the photoelastic constants.

INTRODUCTION

With the development of the multipass Fabry-Perot interferometer¹ Brillouin light scattering has become a useful technique for measuring the elastic properties of opaque polymer rods and polymer films^{2,4}. The frequency of the acoustic phonon as measured with the Brillouin light scattering technique is of the order of 10 GHz, thus making Brillouin scattering a complementary method to ultrasonic studies.

Polymer solids can be oriented by processes such as mechanical stretching or hydrostatic extrusion to improve their mechanical and optical properties. These processes induce elastic deformation as well as forcing the polymer chains to assume a preferred alignment along a particular axis of the solid. The anisotropic elastic properties of oriented polymers are a result of this chain alignment.

In hydrostatic extrusion a cylindrical billet is forced through a heated die by strong hydrostatic pressure. In drawing, a tensile load is applied to the ends of a polymer film which causes the film to stretch. Both methods are known to cause an increase in the elastic stiffness along the orientation axis,^{3,4} but they do not give identical effects. A qualitative comparison of the morphology created by the two deformation processes can be made when all of the elastic constants are known for different degrees of orientation and when samples oriented by both processes have been studied.

The Brillouin light scattering intensity is related to the photoelastic tensor components of solid samples.⁴ The photoelastic constants describe the effect of small elastic deformations on the refractive indices of the

(2)

material.⁷ Thus, it is of interest to look for changes in the photoelastic tensor due to orientation which could then be used to obtain additional information regarding the morphology of the deformed samples.

We have measured the photoelastic tensor components in extruded polypropylene rods using toluene and poly(methylmethacrylate) as the reference scatterers. We have determined the relative photoelastic constants p_{11} , p_{33} , p_{13} and p_{31} in the film samples. The results are used to compare the different morphology produced by the extrusion and drawing processes, and to explain the changes in the spectra due to these deformation processes. We have also measured the elastic constants of polypropylene films drawn to various stretch ratios, and compare the results with the extruded rods. The elastic constants of extruded rods and their connection to the orientation order parameter $\langle P_2(\cos\theta) \rangle$ have already been reported.^{3,4}

EXPERIMENTAL

Polypropylene (PP) films were pressed in a hydraulic press fitted with plates heated to 270°C. The films were melt quenched to limit their crystallinity. Rectangular pieces of film were drawn with a manually operated film puller in a water bath at 80°C. The draw ratio was measured by the separation of marks on the films before and after stretching. Films with draw ratios of 1.0, 3.4, 4.6, 5.8 and 7.3 were prepared. The films were mounted in frames for the light scattering experiments. All film samples are similar in optical quality, being semi-transparent.

The hydrostatic extrusion of PP is described previously.³ The unextruded sample is opaque and thus unsuitable for the elasto-optic study. The extruded samples range in optical quality from translucent at lower ratios to transparent at the highest ratios.

The densities of the film and rod materials were measured in a density gradient column. Both the film and rod densities are found to be unchanged by the deformation processes. The density is .888 g/cm³ for all samples.

The average index of refraction of the PP samples was determined from the angle of critical reflectance at the base of a prism.⁴ Extruded rods of PP can have a birefringence of about .03 at high extrusion ratios.⁸ However, the present refraction index determination method is not sensitive to the birefringence and we have found that each sample has an index equal to 1.49. Thus, assuming this value of birefringence, the errors from our measurements (of sound velocity) will be less than 2%.

The spectrometer consists of a piezoelectrically scanned 5 pass Fabry-Perot from Burleigh Instruments. The incident light is from an Ar ion laser at 4880 Å and made single frequency with an intercavity etalon. The angle

of the incident beam to the collection optics is 90° . The scattered light is detected by a refrigerated photomultiplier tube and the signal current is amplified by a picoammeter and displayed on a chart recorder. The incident polarization is set by a polarization rotor mounted on the laser head. The scattered polarization is chosen with a schlieren-free calcite Glan-Thompson polarizer.

To determine the sound velocity contours in the films, the films are mounted on a goniometer which allows rotation of the films. The film scattering geometry is similar to that used for the poly (ethylene terephthalate) film study, and is shown in Fig. 1. The angle α measured with the goniometer is defined as the angle that the scattering vector (\underline{q}) makes with the z axis (stretch direction) of the film. Thus when $\alpha = 90^\circ$, \underline{q} is along the x axis. The y axis is perpendicular to x and z.

For the photoelastic tensor determination of the extruded rods two samples from each extrusion ratio were cut on a diamond wheel saw. The face geometries are illustrated in Fig. 2.

A poly(methylmethacrylate) (PMM) cube is used as a reference scatterer for determining the photoelastic constants of PP. Faces in a PMM block were cut at 90° to one another and polished to a $.5\mu$ finish. The photoelastic constant P_{1111} for this sample was determined by comparison with a toluene sample whose scattering efficiency is well known.⁹ The PMM is used as a reference here rather than toluene since PMM resembles PP closely in physical and optical properties. The index of refraction of PP and of PMM are nearly the same: $n_{PP} = 1.49$, $n_{PMM} = 1.50$. Thus the correction for internal reflection of scattered light at the sample to air interface is nearly the same in each sample. The external solid angle of collected scattered light will also be nearly the same in each sample.

The scattered intensity from PMM is of the same magnitude as from PP so they can be compared conveniently. Our photoelastic coefficient P_{1111} for PMM is equal to .271.

To compare the scattered intensities of the two samples, the sample is replaced by the reference during the spectrum scan. This minimizes the spectrometer disturbance. The scattering intensity is the integrated intensity and is measured from the area under the Brillouin band.

The PP rod samples of lower extrusion ratio tend to attenuate the laser beam and can depolarize the light as it exits the sample. Therefore, the focussed incident beam is kept as close to the exit surface as possible and the scattered light is collected from the region as close to the entrance face as possible.

RESULTS AND DISCUSSION

Figure 3 shows the Brillouin spectra of the $R_s = 3.4$ and $R_s = 7.3$ films where $\alpha = 45^\circ$. The high frequency band is the scattering from the quasi-longitudinal (QL) wave and the low frequency one is the scattering from the quasi-transverse (QT) wave. Note the increase in the QT scattered intensity at higher draw ratio. There are additional Brillouin components present in the spectra. They are due to the internal reflection in the film samples, as has been described previously.⁵

In a birefringent medium the hypersonic velocity V_s is related to the Brillouin frequency shift, f_B , by:

$$V_s = f_B \lambda_i / (n_u^2 + n_u'^2 - 2n_u n_u' \cos \theta) = f_B / q \quad (1)$$

where λ_i is the incident wavelength and θ is the scattering angle n_u and n_u' are the indices of refraction along the incident and scattered directions.

For the scattering geometry illustrated in Fig. 1 where the film bisects

(6)

the 90° laboratory scattering angle, Equation (1) simplifies to²:

$$V_s = f_B \lambda_i / \sqrt{2} \quad (2)$$

This simplification is convenient for studying the polymer films where it is difficult to measure the refractive index, since in this geometry it is unnecessary to know the variation of refractive index to determine the sound velocity.

A uniaxial deformation process such as stretching or extrusion changes the symmetry of an unoriented isotropic solid to a uniaxial or the equivalent hexagonal symmetry. These oriented polymer samples possess the elements of the high symmetry H_1 class. The elastic constant tensor for hexagonal symmetry has the form¹⁰:

$$C_{ijkl} = \begin{bmatrix} C_{11} & C_{12} & C_{13} & 0 \\ C_{12} & C_{11} & C_{13} & \\ C_{13} & C_{13} & C_{33} & \\ & & & C_{44} \\ & & & C_{44} \\ & 0 & & \\ & & & C_{66} \end{bmatrix} \quad (3)$$

and the photoelastic tensor:

$$P_{ijkl} = \begin{bmatrix} P_{11} & P_{12} & P_{13} & 0 \\ P_{12} & P_{11} & P_{13} & \\ P_{31} & P_{31} & P_{33} & \\ & & & P_{44} \\ & & & P_{44} \\ & 0 & & \\ & & & P_{66} \end{bmatrix} \quad (4)$$

where $C_{66} = \frac{1}{2}(C_{11} - C_{12})$ and $P_{66} = \frac{1}{2}(P_{11} - P_{12})$. The contracted subscript notation⁷ of Voight is used for both C_{ijkl} and P_{ijkl} .

(7)

If the elastic constants tensor is substituted in the equations of motion (neglecting the damping) for a solid, we obtain the Christoffel equation for hexagonal symmetry¹¹:

$$\begin{bmatrix} (c_{11}\ell_x^2 + c_{66}\ell_y^2 + c_{44}\ell_z^2) - \rho V^2 & (c_{12} + c_{66})\ell_x\ell_y & (c_{13} + c_{44})\ell_x\ell_z \\ (c_{66}\ell_x^2 + c_{11}\ell_y^2 + c_{44}\ell_z^2) - \rho V^2 & (c_{12} + c_{66})\ell_y\ell_z & (c_{13} + c_{44})\ell_y\ell_z \\ (\text{symmetric}) & (c_{44}\ell_x^2 + c_{44}\ell_y^2 + c_{33}\ell_z^2) - \rho V^2 & (c_{44}\ell_x^2 + c_{44}\ell_y^2 + c_{33}\ell_z^2) - \rho V^2 \end{bmatrix} \begin{bmatrix} U_x \\ U_y \\ U_z \end{bmatrix} = 0 \quad (5)$$

where ρ is the density, V is the velocity of the sound wave, the U_k are the particle displacement components and the ℓ_k are the direction cosine components of scattering vector q along the x , y and z axes. The amplitude of q is defined in Eq. (1).

The sound velocity contours of the quasilongitudinal (QL) and quasi-transverse (QT) waves measured from the Brillouin spectra at different propagation directions in the films are plotted in Fig. 4. To obtain the elastic constants⁵ c_{11} , c_{33} , c_{44} and c_{13} from these sound velocity contours, we used a least squares computer fitting routine to fit our experimental points to Eq. (5) for the case where the propagation direction is in the $x-z$ plane:

$$2\rho V_{\pm}^2 = (c_{11}\ell_x^2 + c_{33}\ell_z^2 + c_{44}) \pm \{(c_{11}\ell_x^2 + c_{33}\ell_z^2 + c_{44})^2 - 4[(c_{11}\ell_x^2 + c_{44}\ell_z^2) - \ell_x^2\ell_z^2(c_{13} + c_{44})]\}^{1/2} \quad (6)$$

where the + and - roots correspond to the QL and QT waves, respectively, and the components $\ell_x = \sin \alpha$, $\ell_z = \cos \alpha$ are measured from the goniometer;

The solid curve through the data points in Fig. 4 is the fit to Eq. (6).

The elastic constants c_{11} , c_{33} , c_{44} and c_{13} obtained from the fitting are plotted versus draw ratio in Fig. 5. The largest change is seen in c_{33} which increases linearly with deformation ratio. c_{11} decreases as the undrawn film is first stretched and then stays constant at higher draw ratio. c_{44} is unchanged by orientation and c_{13} increases linearly with deformation.

Comparison of the elastic constants of the stretched films with that of extruded rods (Ref. (4)) are also given in Fig. 5. For poly(propylene) the draw ratio defined according to the linear dimension of the films is quantitatively equal to the extrusion ratio of the extruded rod, as the volume of polypropylene remains unchanged by deformation. However, the trends of the elastic constants here are different from those in the films. The increase in C_{33} of the extruded rod with deformation ratio is non-linear, and C_{11} decreases with deformation ratio. C_{44} is again constant and C_{13} appears to decrease slightly with extrusion.

It is apparent that PP responds differently to the two deformation processes. The magnitude of change in C_{33} is larger in the stretched film which would indicate that the chain extension in the deformation direction is greater in the oriented films. The trend of C_{13} is different in the film and rod samples. C_{13} is a measure of the efficiency of a compressional stress along the x axis for creating a strain along the z axis. An increase in C_{13} with deformation suggests that the chains are extended in the stretch direction. A decrease in C_{13} suggests that the polymer chains are folded by extrusion so that short segments rather than a full extension of the chain are aligned along the extrusion axis. The linkage between a stress along x and the resultant strain along z is weakened by the presence of folds in the chains.

It should be noted that the error in measurement of C_{13} in the rod samples is much larger than in the film samples. It is possible to increase the accuracy of measurement for the rod samples by cutting flat slices of the extruded rods so that the slices contain the z axis then studying these samples in the same manner as the films. Since the LAM bands present at low frequency in the Raman spectrum of polymer samples is a sensitive

(9)

indicator of the distribution of chain lengths in polymers,^{12,13} studies of the change in the lineshape of the LAM bands will provide useful information about the chain folding process as revealed in the change of C₁₃. We plan to carry out further studies of extruded and stretched polymers using both of these techniques.

The photoelastic tensor is defined by the change in the inverse dielectric tensor $\delta\epsilon_z^{-1}$ as (the summation convention with repeated indexes indicating summation is implied throughout this paper)

$$(\delta\epsilon_z^{-1})_{ij} = p_{ijkl} \frac{\partial U_k}{\partial X_l} \quad (7)$$

where $\frac{\partial U_k}{\partial X_l}$ is the displacement gradient associated with the sound wave. The photoelastic tensor p_{ijkl} is symmetric with respect to i and j but not necessarily symmetric with respect to k and l, due to the contribution of rotations of the volume element in an optically anisotropic medium.¹⁴ For hexagonal symmetry, the components that are affected by this condition are p₂₃₂₃ and p₂₃₃₂, which in contracted notation corresponds to p₄₄ and p_{4̄4}. However, in the present work the scattered intensity of the shear wave from which p₄₄ and p_{4̄4} would be measured is below our detection limit.

The integrated intensity of the Brillouin scattered light associated with the acoustic phonon with scattering wave vector q, excited with incident polarization \hat{e}_μ and scattered polarization $\hat{e}_{\mu'}$, is given by

$$I_{\mu\mu'}(q) = A \langle |\delta\epsilon_{\mu\mu'}(q)|^2 \rangle \quad (8)$$

where A is a constant and $\delta\epsilon_z$ is the fluctuation in the dielectric constant tensor, given by:

$$\delta\epsilon_{\mu\mu'}(q) = \int e^{iq \cdot r} \delta\epsilon_{\mu\mu'}(r) d^3r. \quad (9)$$

The $\delta\epsilon_z$ tensor is related to the $\delta\epsilon_z^{-1}$ tensor by

$$\delta\epsilon_{\mu\mu'} = -\epsilon_0 \epsilon_{\mu i} \epsilon_{\mu' j} (\delta\epsilon_z^{-1})_{ij} \quad (10)$$

(10)

where ϵ^o is the equilibrium dielectric tensor $\epsilon_{\mu i}^o$ and $\epsilon_{\mu' j}^o$ and are related to the principal refractive indices

$$\epsilon_{\mu i}^o = n_i^2 e_{\mu, i}; \quad (11)$$

$e_{\mu, i}$ is the component of the polarization vector \hat{e}_{μ} projected along the i th principal axis; n_i are the principal refractive indices. Using Eqs. (7), (9), (10), and (11) we can rewrite Eq. (8) as

$$I_{\mu\mu'}(q) = A n_i^2 n_j^2 e_{\mu, i} e_{\mu', j} \langle |B_{ij}|^2 \rangle \quad (12)$$

where:

$$B_{ij} = P_{ijkl} U_k q_1. \quad (13)$$

We define the scattering factor $\beta_{\mu\mu'}^6$ as:

$$\beta_{\mu\mu'}^6 = \left(\frac{1}{4}\right)^6 \frac{n_i^2 n_j^2 e_{\mu, i} e_{\mu', j} \langle |B_{ij}|^2 \rangle}{\rho V_s^2} \quad (14)$$

where n_{μ} and $n_{\mu'}$ are respectively the index of refraction associated with the incident and scattered radiation. The scattering factor determines the intensity of a given Brillouin band.⁶

Four scattering geometries are used to measure the photoelastic tensor components in the rod samples. These geometries are illustrated in Fig. 2, along with the respective scattering factor expressions calculated from Eq. (14). The photoelastic tensor components are then determined by fitting the experimental relative intensity results to Eq. (14). The result for the photoelastic tensor components which we have obtained for the various extrusion ratios are plotted versus extrusion ratio in Fig. 6. One notes that the values of P_{13} and P_{31} are not equal; furthermore, the values of P_{13} , P_{31} and P_{12} are seen to be unaffected within the experimental error by the extrusion process. P_{11} , P_{33} and P_{66} should in principle be measurable from the rod samples, however, due to the weak depolarized intensity, the uncertainty in these values is quite large.

For the film samples the intensity of the QL and QT Brillouin lines for scattering where q is in the $x-z$ plane, is determined by the scattering factor

(neglecting the birefringence)

$$S_m = (\rho V_{m,\alpha}^2)^{-1} [(p_{11} U_x \sin \alpha + p_{13} U_z \cos \alpha) \cos^2 \alpha + (p_{33} U_z \cos \alpha + p_{31} U_x \sin \alpha) \sin^2 \alpha]. \quad (15)$$

The U_x and U_z are the displacement eigenvectors of Eq. (5) which for wave propagation in the x-z plane of the sample are given by:

$$(C_{11} \sin^2 \alpha + C_{44} \cos^2 \alpha - \rho V_{m,\alpha}^2) U_x = [(C_{13} + C_{44}) \sin \alpha \cos \alpha] U_z. \quad (16)$$

The subscript m refers to the QL or QT wave and ρV_{α}^2 is determined at each angle, α , in the film.

The ratios of the QL and QT scattered intensities can be experimentally determined from the film spectra at several angles in the x-z plane of the film. The ratio of the scattering factors $\beta(QT)/\beta(QL)$ are plotted versus angle in Fig. 7. The ratio $\beta(QT)/\beta(QL)$ reaches a maximum at $\alpha \approx 45^\circ$ for each drawn film. The value of maximum $\beta(QT)/\beta(QL)$ also increases with the draw ratio.

The relative values of p_{11} , p_{33} , p_{13} and p_{31} are extracted from the intensity ratio data by forming the ratio of $\beta(QT)/\beta(QL)$ from Eqs. (15) and (16). We then determined the values of the p_{ij} which best fit this equation to the experimental ratios using a least squares computer fitting program. The solid curves in Fig. 7 are the curves fitted to the experimental data points.

The relative values of the p_{ij} from the fitting are plotted versus draw ratio in Fig. 6. The values of p_{11} , p_{33} , and p_{13} are shown relative to p_{31} since the experimental values of p_{31} shows the least variation in the rod samples. The relative value of p_{33} increases with the degree of deformation to a draw ratio of about 5, whereas the relative value of p_{11} decreases slightly. The relative value of p_{13} follows the value of p_{31} , which is held as a reference.

We estimate the error in measuring the relative photoelastic constants in the film samples to be about 10% and the error in the rod sample measure-

ments to be about 15%. The increase in P_{33} as well as the decrease in P_{11} as observed in the films are greater than the experimental uncertainty limits.

In the rod samples there is no change in the photoelastic tensor components P_{13} , P_{31} , and P_{12} within the experimental error. The relative value of P_{31} and P_{13} in the films also does not change with stretching. We conclude therefore that stretching of a polymer sample causes a small increase in P_{33} and a smaller decrease in P_{11} , while the values of P_{12} , P_{13} , and P_{31} are unaffected by the deformation.

The theory of the photoelastic interaction in non-ferroelectric media has been formulated by Nelson and Lax.¹⁵ The photoelastic susceptibility of the symmetric part of the photoelastic effect is given by a sum of 3 terms. The first term is from the change in the number of oscillators per unit volume due to compression and dilation effects from longitudinal acoustic waves. Since stretching or extrusion does not affect the density of PP this term is not expected to vary significantly with degree of chain alignment. The second term arises from a direct mixing of the optic and acoustic fields. There are two cases to be considered here: 1) the acoustic and optic waves share a common internal coordinate. In this case, the contribution to the photoelasticity arises from the deformation-altered resonant frequency. This term will be affected by the polarizability of the microscopic units along the x and z axes of the samples and the effects of this term are expected to appear in P_{11} and P_{33} ; 2) when the acoustic and optic fields do not have a common internal coordinate, there is a contribution from the deformation-altered oscillator strengths arising from the optic and acoustic field interaction. This term applies to P_{13} , P_{31} , and P_{12} . Since these quantities do not change with the degree of chain alignment the interaction of the optic and acoustic fields is not

significantly affected by the degree of chain alignment. We shall not consider the third term in this discussion since it is an indirect effect and of higher order.

It is now apparent that the photoelastic constants are not the factors which cause the changes in the Brillouin scattering intensity as the polymer samples are uniaxially deformed. In the expression for the scattering factors for QL and QT wave propagation (cf. Eqs. (15) and (16)) we see the scattering factors are also affected by two other variables: the component of the unit displacement vectors; \hat{U} , and the "directional" elastic constant, ρV_a^2 . Each of these variables is a function of the four elastic constants and hence changes with the degree of deformation.

Shown in Table I are the unit displacements for sound propagation along (1 0 1) ($\alpha = 45^\circ$) in the oriented films for QL and QT. There is a change in the displacements due to the changes in the elastic constants. The changes in the particle displacement vectors are thus one of the factors that cause the variation of scattered intensity from the QL and QT waves.

The directional elastic constant, ρV_a^2 , is a variable which also changes with deformation ratio. To find the effect of the change of this variable one can study a phonon which propagates in a pure mode direction. For the pure longitudinal mode direction the displacement is in the direction of propagation, and thus the displacement for this phonon will not be affected by deformation.

Table II lists the intensity ratio of the PP sample and the PMM standard for each sample. There is an increase with extrusion ratio in the scattered intensity from the (1 0 0) phonon. In this case, the increase in intensity is due to the change in C_{11} , which according to Fig. 5 decreases with extrusion ratio. Since C_{11} is in the denominator of the scattering factor (cf. Eq. (15)),

the increase in the scattered intensity at higher deformation is associated with the decrease in this elastic constant.

In conclusion, it appears that different kinds of morphology are produced by stretching and extrusion of PP. The elastic constants of the film samples are affected more by the extended chains whereas the change in the elastic constants of the extruded samples suggests that short-segment alignment and chain folding are the dominant feature in the morphology of the extruded samples.

The photoelastic constants p_{11} and p_{33} affected by stretching in the films. The changes are due to a resonant interaction between the optic and acoustic fields through the polarizability of the oriented polymer. The photoelastic constants p_{12} , p_{13} , and p_{31} are unaffected by orientation. The intensity changes in the Brillouin spectra are due mainly to the change in the elastic constants which appear in the particle displacements, rather than to the change in the photoelastic constants.

Acknowledgement:

We acknowledge the financial support of the Chemistry Program of the Office of the Naval Research and of the NSF polymer program (Grant No. DMR 79-12457) for this research.

REFERENCES

- 1) J. Sandercock in Light Scattering in Solids (Flammarion, Paris, 1971, pp. 9-12).
- 2) C.H. Wang, D.B. Cavanaugh, and Y. Higashigaki, *J. Polym. Sci. (Phys. Ed.)* (in press).
- 3) D.B. Cavanaugh and C.H. Wang, *Macromolecules* (in press).
- 4) C.H. Wang and D.B. Cavanaugh, *J. Applied Phys.* (in press).
- 5) D.B. Cavanaugh and C.H. Wang, *J. Applied Phys.* (in press).
- 6) R. Vacher and L. Boyer, *Phys. Ref. B*, 6 (2), 639, (1972).
- 7) A. Feldman, *Optical Engineering*, 17, (5), (1978).
- 8) T. Williams, *J. Material Sci.*, 8, 59, (1973).
- 9) I.L. Fabellinski, Molecular Scattering of Light (Plenum, New York, 1968, p. 563).
- 10) J.F. Nye, Physical Properties of Crystals, (Clarendon, Oxford, 1960).
- 11) B.A. Auld, Acoustic Waves and Fields in Solids. I, (John Wiley and Sons, New York, 1973).
- 12) R.G. Snyder, S.J. Krause, J.R. Scherer, *J. Polymer Sci., Polym. Phys.*, 16, 1593, (1978).
- 13) R.G. Snyder, J.R. Scherer, *J. Polym. Sci., Polym. Phys.*, 18, 421, (1980).
- 14) D.F. Nelson, M. Lax, *Phys. Rev. Lett.*, 24 (8), 379, (1970).
- 15) D.F. Nelson, M. Lax, *Phys. Rev. B*, 3(8), 2778, (1971).

FIGURE CAPTIONS

1. The film scattering geometry used in the present study. The angle α is defined as the angle between the scattering vector and the stretch axis of the film.
2. The face geometries used in the determination of the photoelastic tensor components for rod and film samples.
3. Brillouin spectra of the film stretched to $R_s = 3.41$ and $R_s = 7.3$ at $\alpha = 45^\circ$.
4. Sound velocity contours of the quasilongitudinal (QL) and quasitransverse (QT) waves plotted in polar coordinates measured from the Brillouin spectra at different propagation directions.
5. The elastic constants of poly(propylene) films plotted as a function of draw ratio. The elastic constants of extruded rods reported in ref. 3 are also included for comparison. Solid points - stretched films, open points - extruded samples.
6. The photoelastic constants plotted versus deformation ratio:
 - a) film samples \blacklozenge - p_{33} \blacktriangle - p_{11} \circ - p_{31} \textcirclearrowright - p_{13}
 - b) extruded samples \bullet - p_{31} \square - p_{12} \circ - p_{13}The estimated error is indicated for each sample type.
7. Ratio of the scattering factors for the quasilongitudinal and for the quasitransverse acoustic modes. \bullet - $R_s = 7.3$ \circ - $R_s = 5.8$
 \blacksquare - $R_s = 4.6$ \blacktriangle - $R_s = 3.4$. The solid curves are calculated from the p_{ij} values.

Captions (cont)

Table I: The unit displacement vectors at $\alpha = 45^\circ$ in the stretched samples;
 R_s is the stretch ratio.

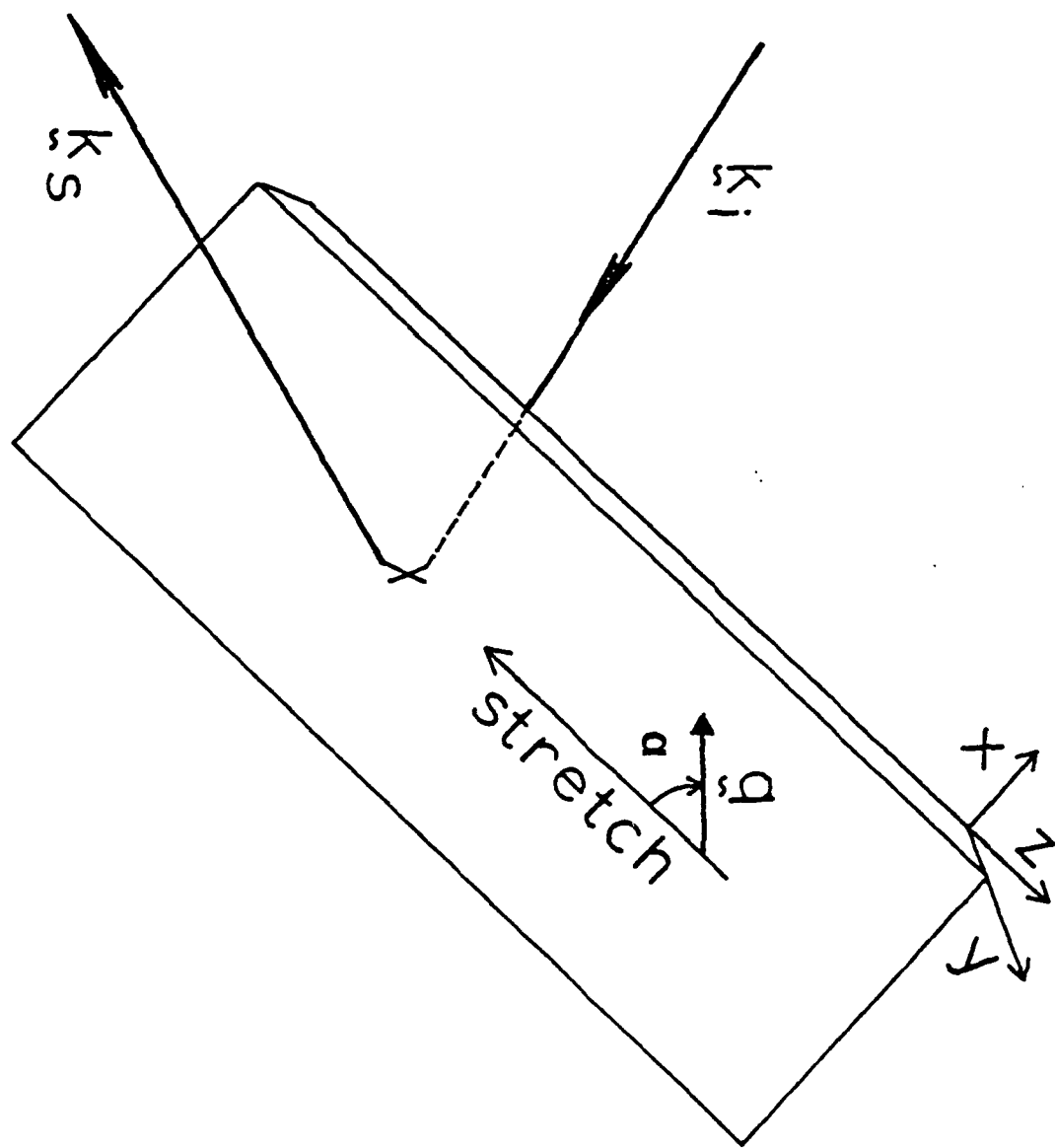
Table II: The intensity ratio of the longitudinal (1 0 0) phonon in extruded
PP to the PMM standard; R_E is the extrusion ratio.

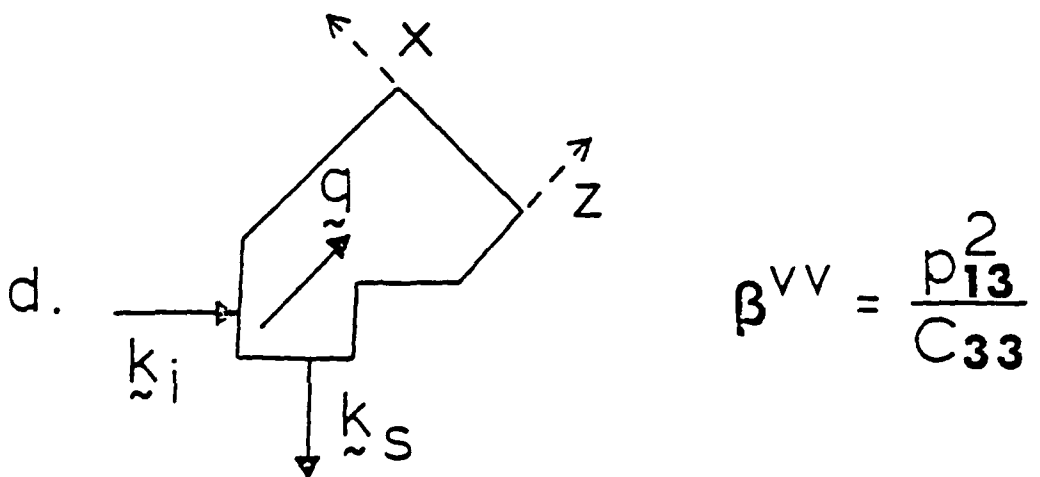
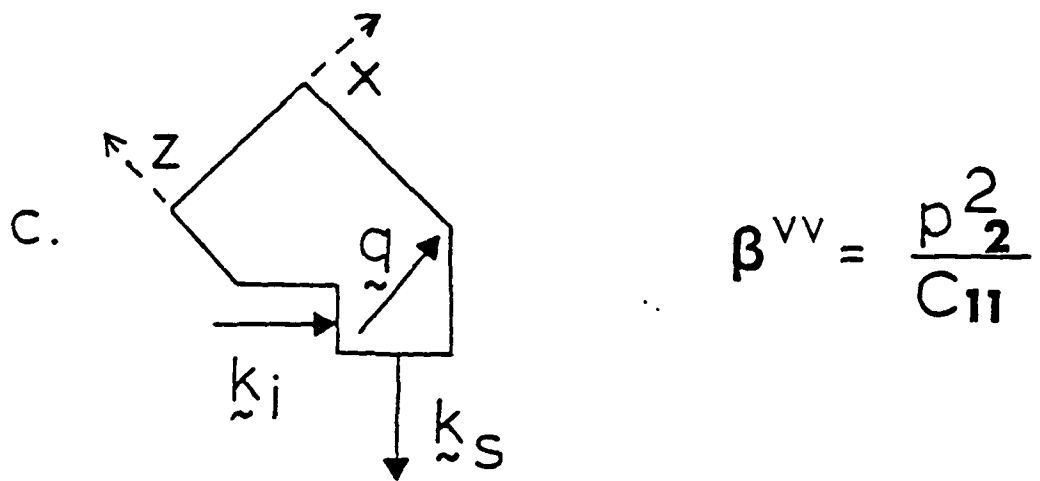
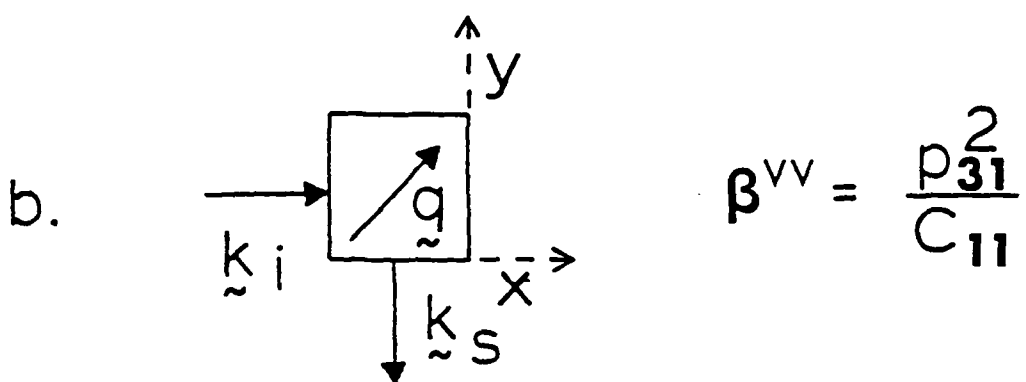
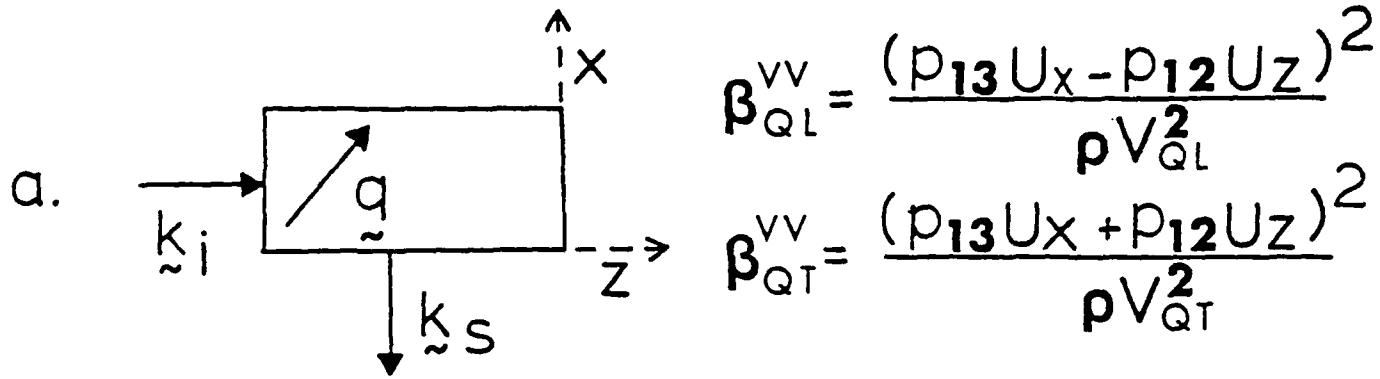
Table I

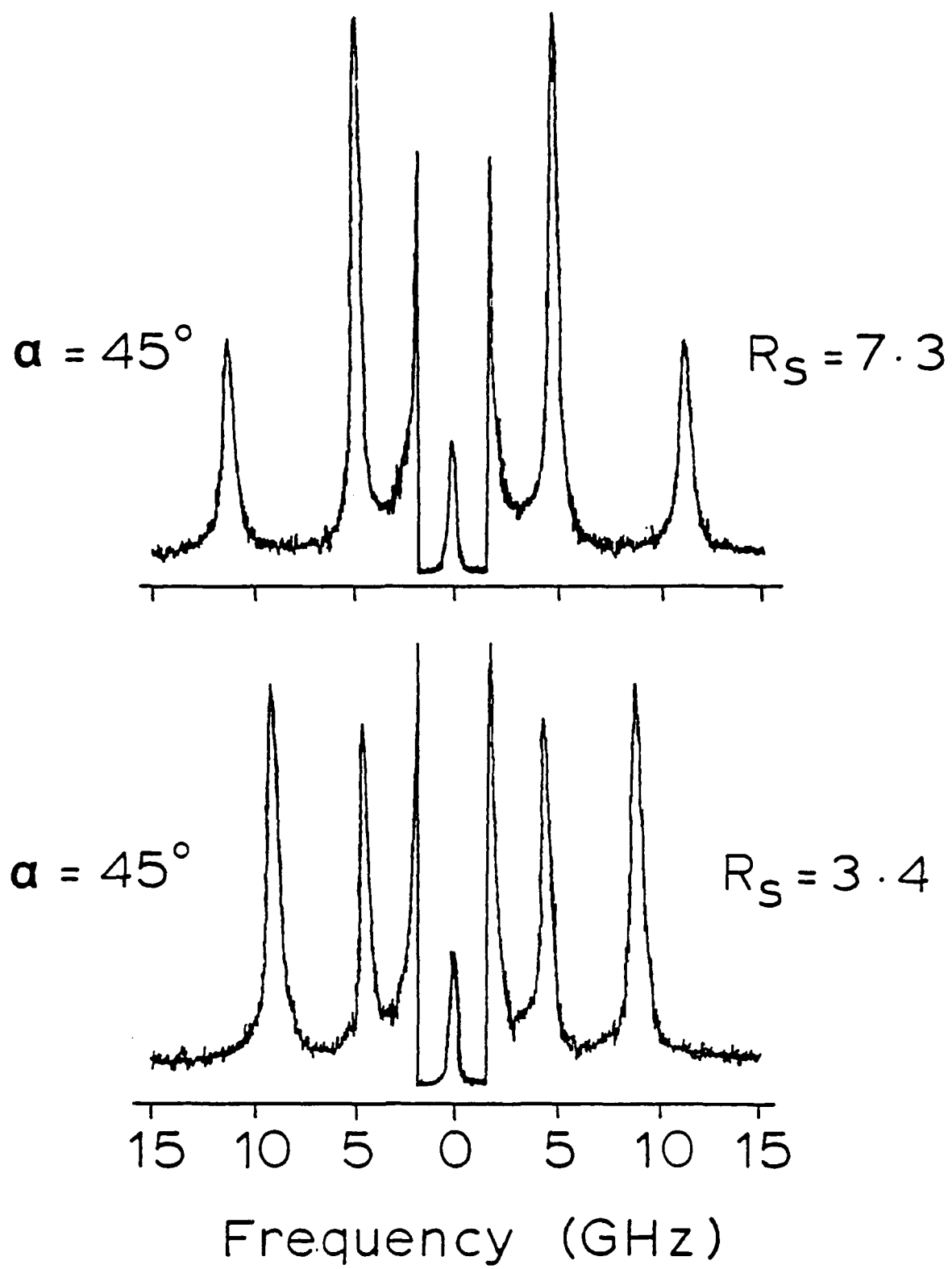
<u>R_s</u>	<u>Quasilongitudinal</u>		<u>Quasitransverse</u>	
	<u>U_x</u>	<u>U_z</u>	<u>U_x</u>	<u>U_z</u>
1.0	.7071	.7071	-	-
3.4	.4081	.9129	-.9129	0.4081
4.	.3636	.9316	-.9316	.3636
5.	.3196	.9476	-.9476	.3196
7.3	.2780	.9606	-.9606	.2780

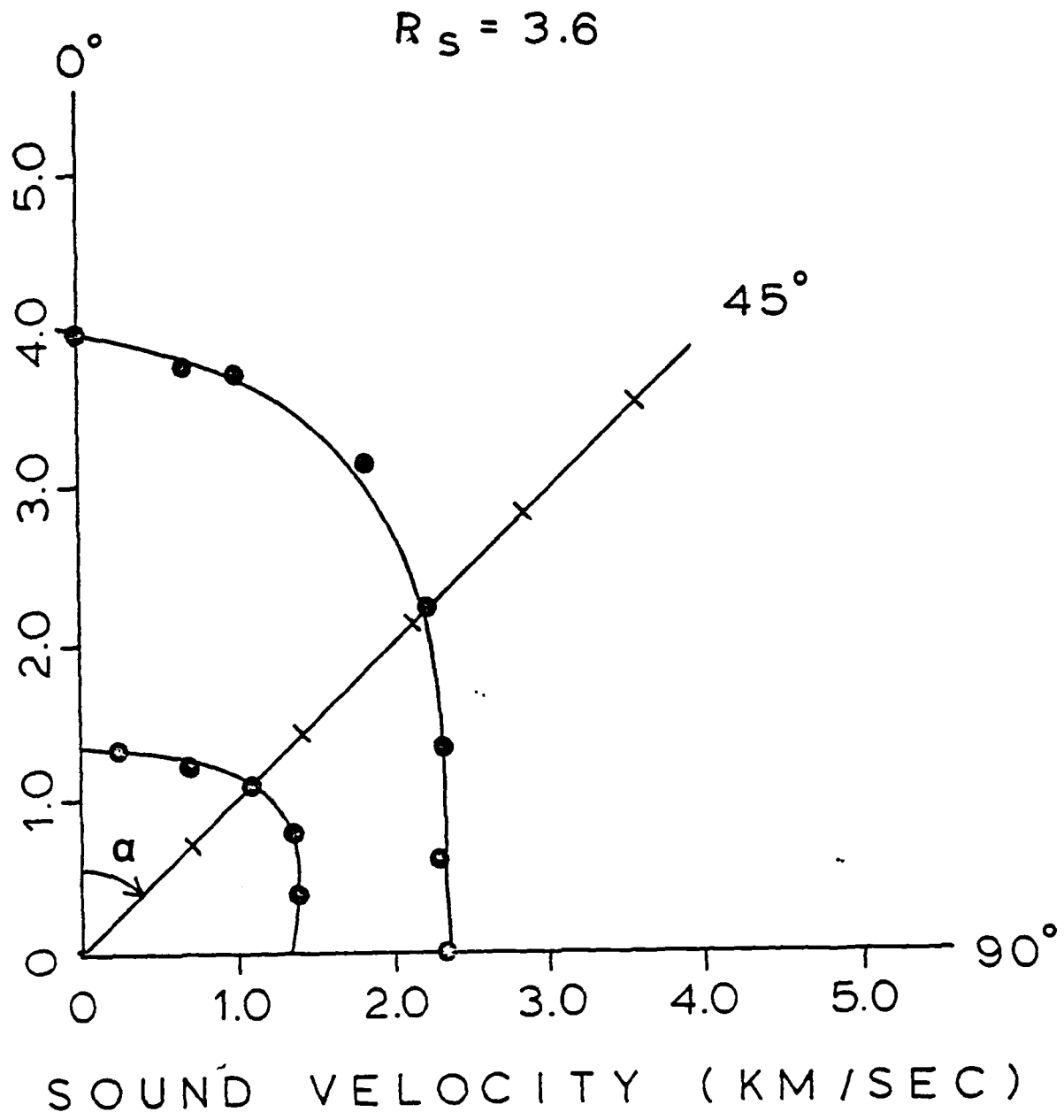
Table II

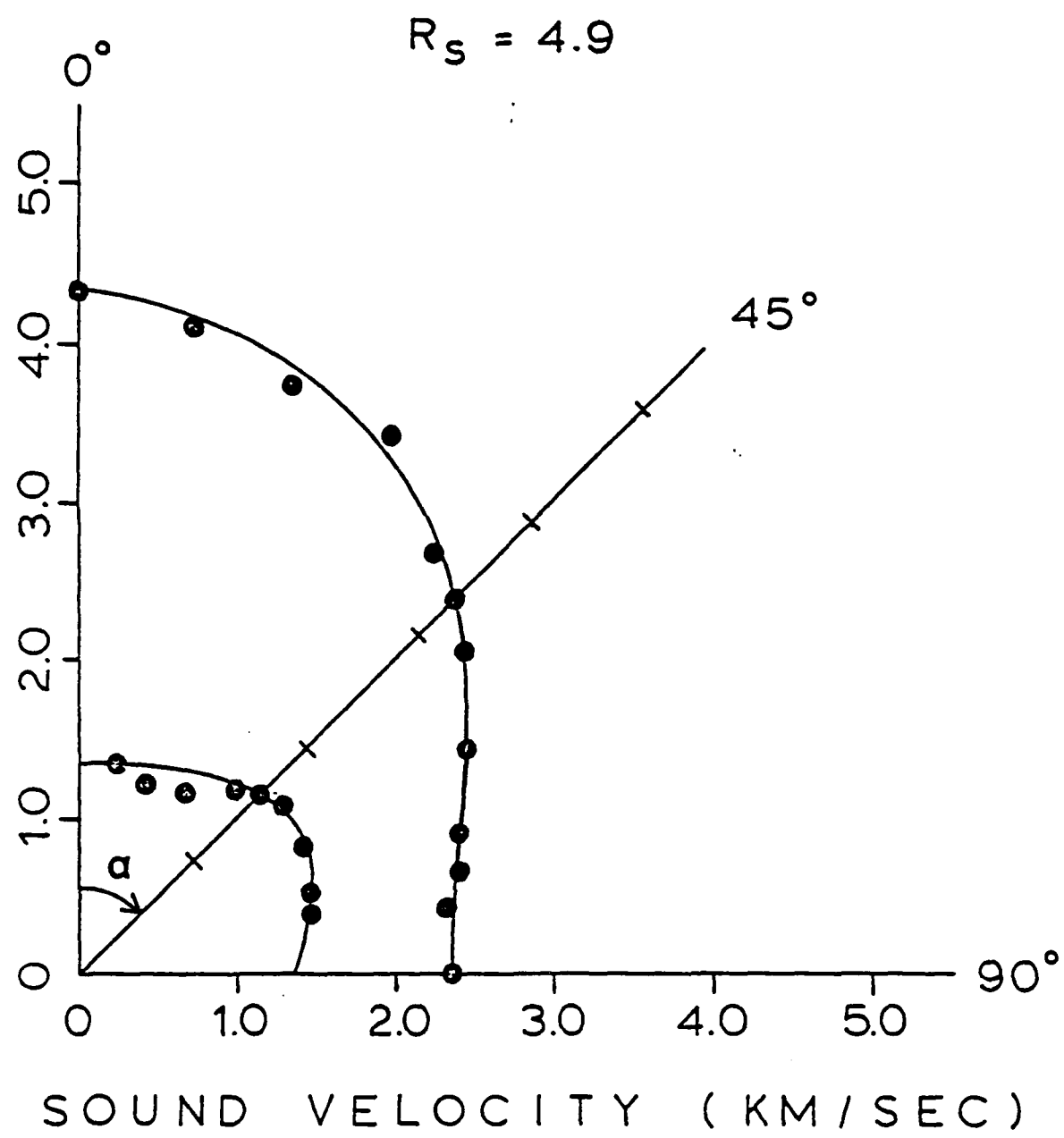
<u>RE</u>	<u>$\beta_{(PP)}/\beta_{(PMM)}$</u>
3.0	.996
3.4	.952
4.8	1.20
6.3	1.40

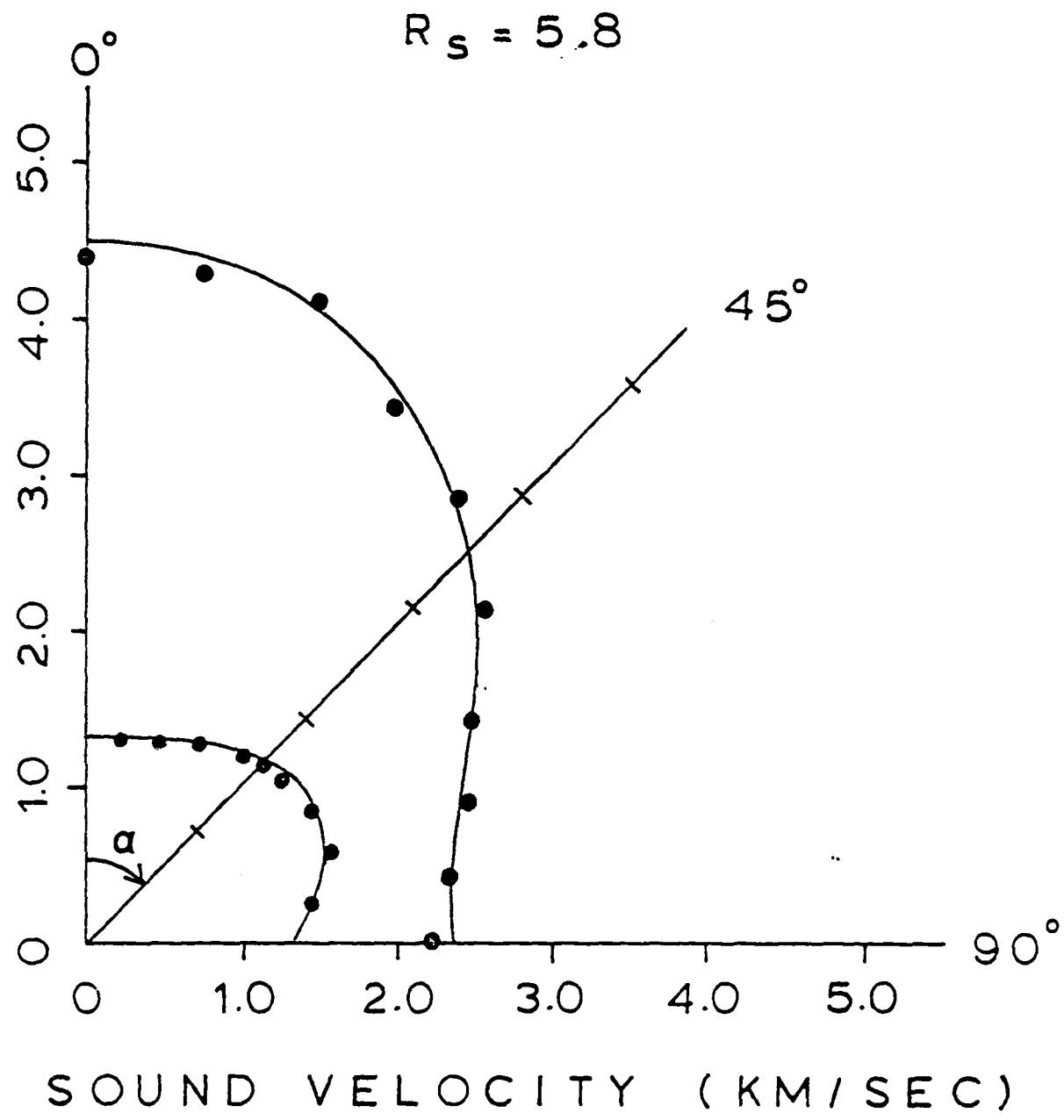




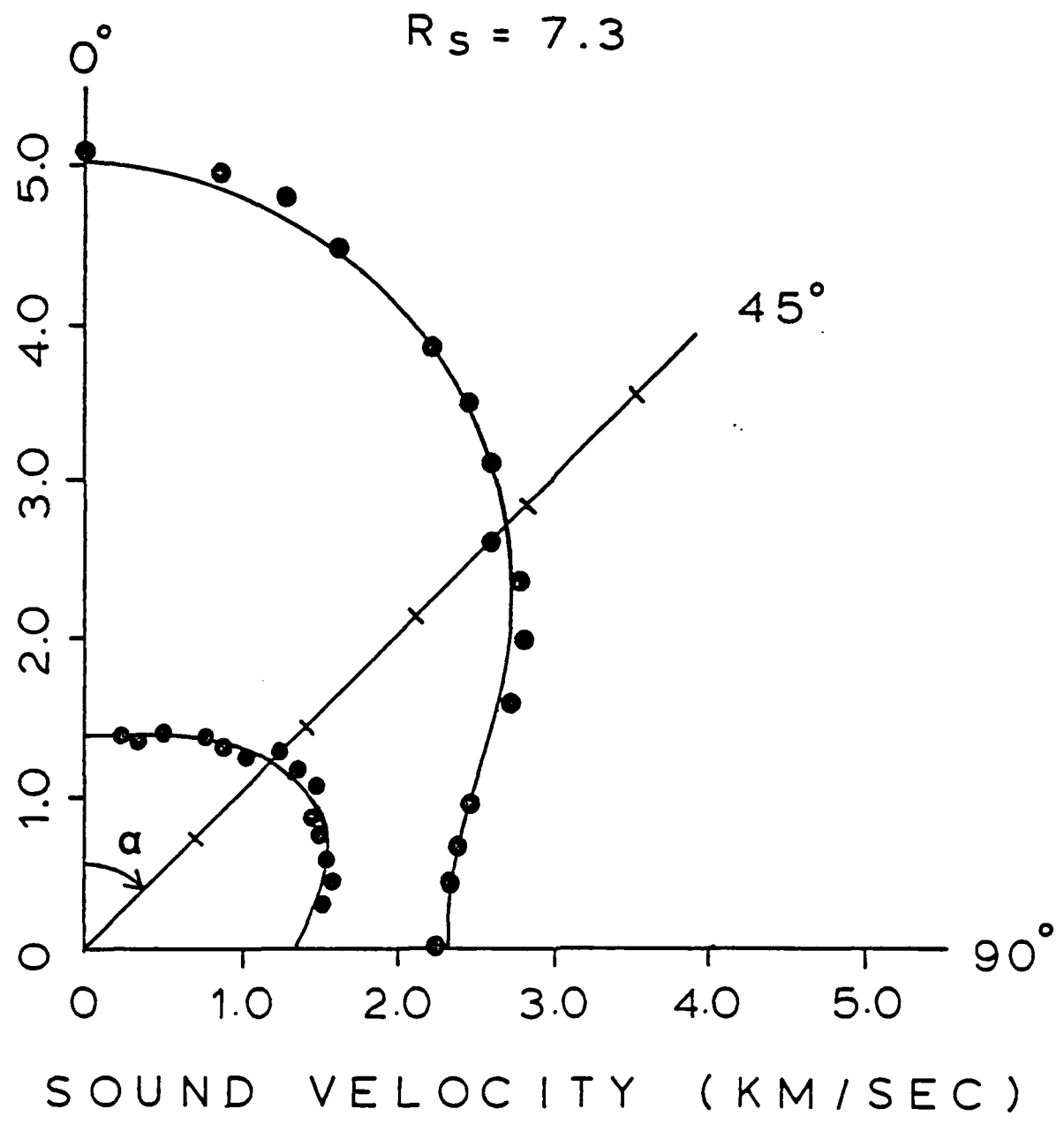




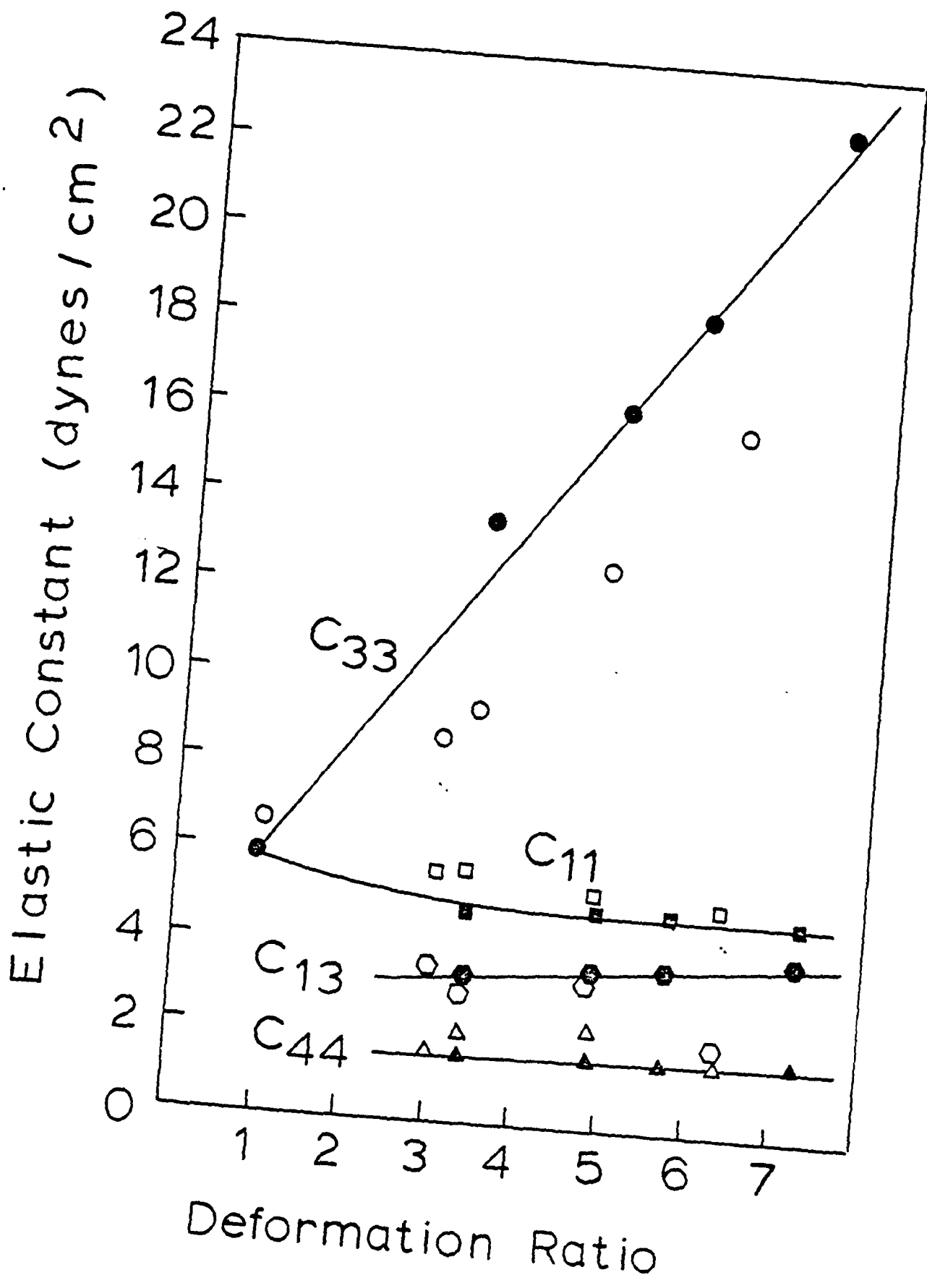




-c



4d



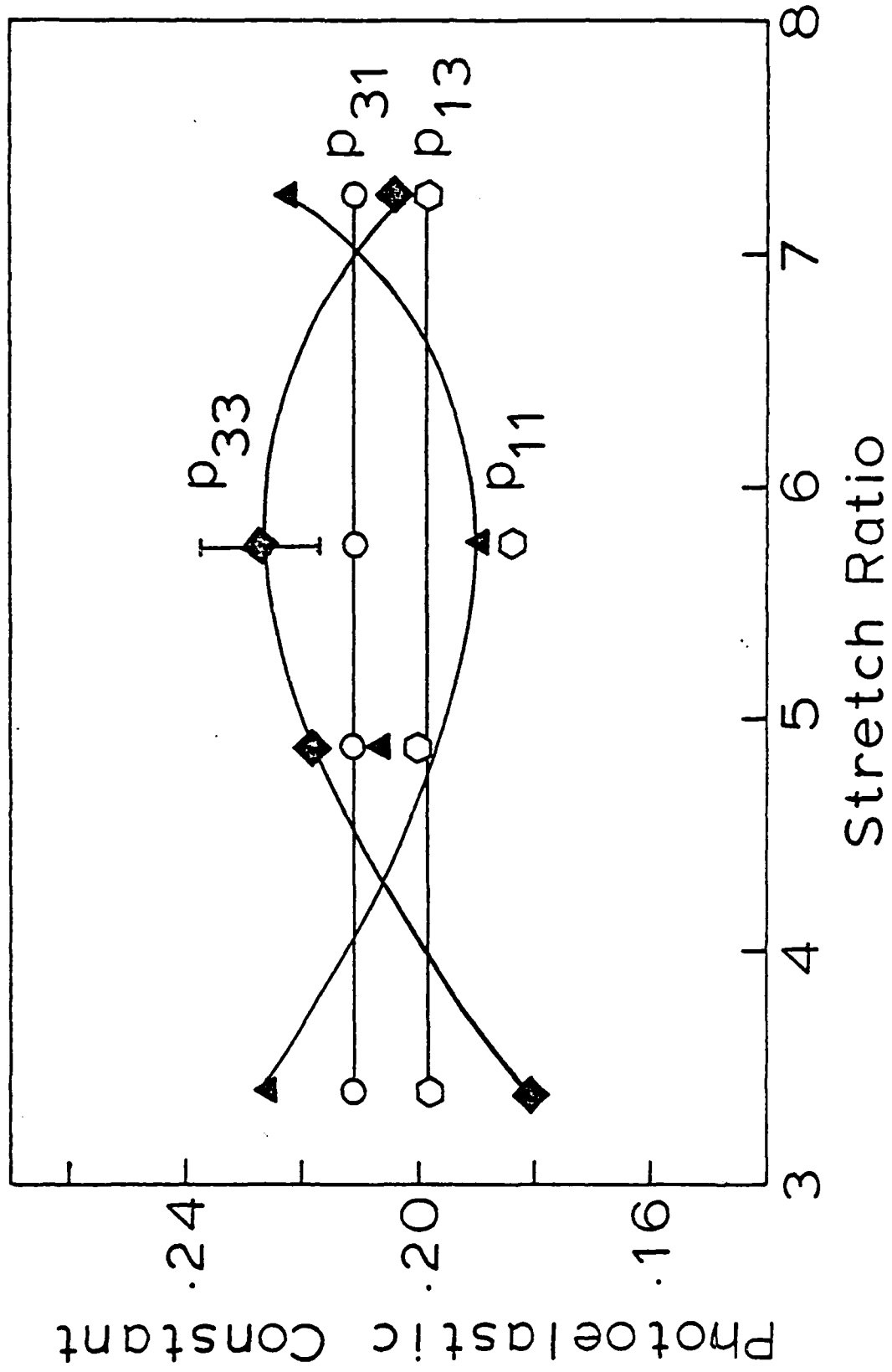
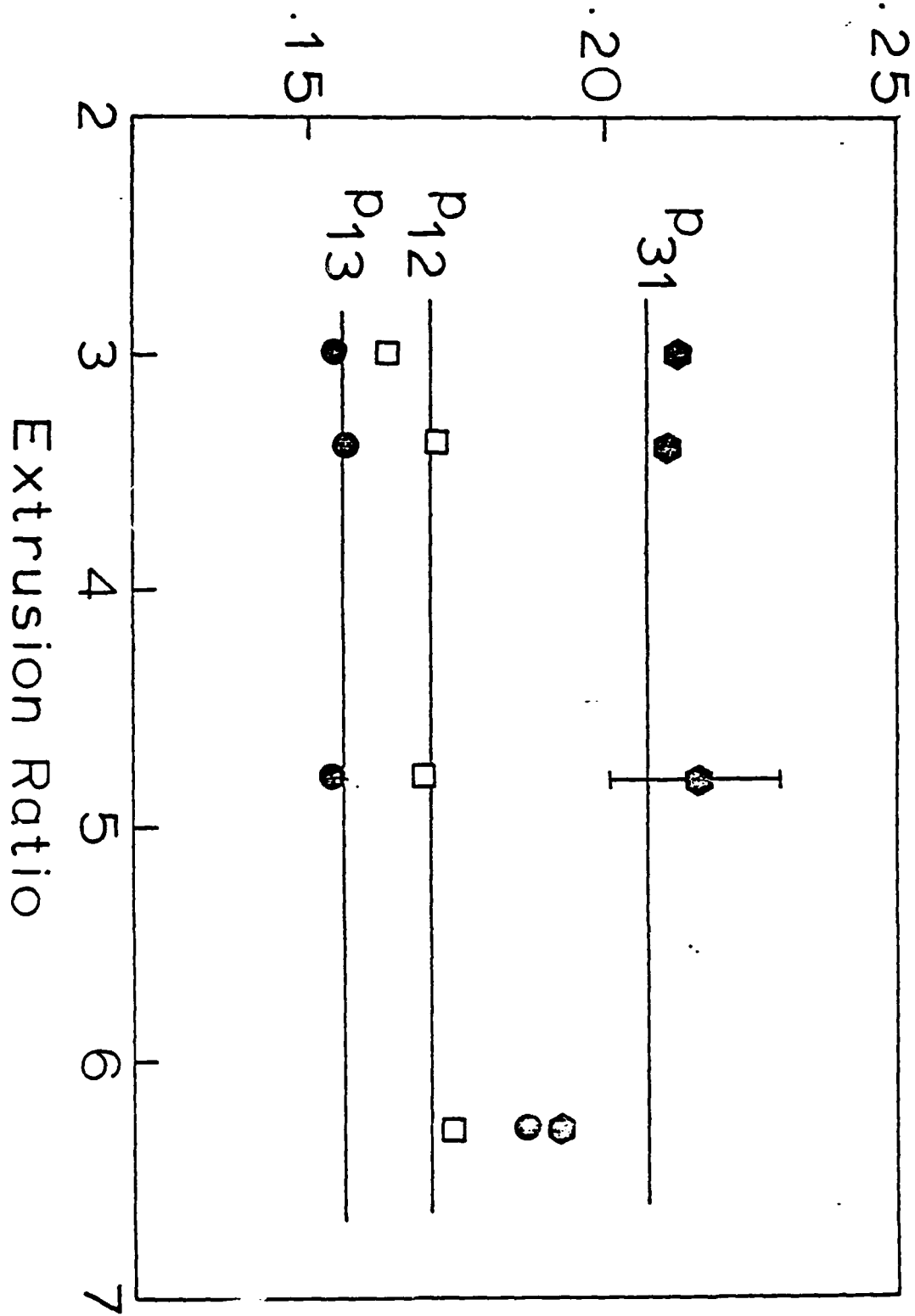


Fig 6 a

Photoelastic Constant



β_{QT} / β_{QL}

